

# On-axis irradiance for spherically aberrated optical systems with obscured rectangular apertures: a study using the Wigner distribution function

WALTER D. FURLAN, GENARO SAAVEDRA,  
ENRIQUE SILVESTRE and MANUAL MARTINEZ-CORRAL  
Departamento de Óptica, Universitat de València, Moliner 50,  
E-46100 Burjassot, Spain

(Received 13 February 1997)

**Abstract.** The assessment of optical focusing systems with obscured rectangular pupil masks suffering from spherical aberration is performed by use of a novel technique for the computation of the irradiance distribution along the optical axis. It is shown that all the values of this function for a variable spherical aberration can be obtained from a single bidimensional phase-space representation: a Wigner distribution function associated with the pupil function of the system. Several numerical examples illustrating the behaviour of such aberrated systems are presented and some interesting features of the results are discussed.

## 1. Introduction

The study of the properties of the axial component of the far-field irradiance distribution corresponding to a purely-absorbing pupil filter has deserved the attention of many researchers over the past few years. This study contemplates several interesting aspects like the focal-shift effect that is inherent to the low Fresnel-number focusing systems [1-3], the symmetries and periodicities of the axial field [4], and the effect of annular [5], apodizing [6], or super-resolving [7-9] pupil filters on the profile of the axial irradiance distribution. Moreover, the on-axis image irradiance is an essential merit function from which several quality criteria, such as the Strehl ratio versus defocus, can be obtained [10]. The effect of the primary spherical aberration on the axial irradiance has been explored theoretically and experimentally for both unobscured [11] and obscured [12] rotationally symmetric systems.

On the other hand, the far-field axial irradiance concentration is an important parameter in the study of unstable laser resonators. These devices provide an output beam that, in general, is uniform in amplitude and spherical in phase across an annular, or obscured square aperture. The edges of the aperture have major effects on the outgoing wave in producing strong diffraction effects that can only be taken into account by performing a full diffraction study. In this sense, some studies of the far-field properties for various models of unstable resonators have been reported for non-centrally obscured circular and square apertures [13-16]. Nevertheless, little attention has been paid to the effect of the spherical aberration in such systems. This is an unexpected fact since this aberration is inherent to devices consisting of spherical mirrors.

Our aim in this paper is to evaluate the influence of spherical aberration in the focusing properties of unstable optical resonators. In particular, we focus our attention on the particular class of astigmatic rectangular unstable resonators characterized by a square aperture obscured by a rectangular non-centred mask. These setups are interesting because of their high tolerance to misalignments [17].

For the above analysis, we propose a new method for the efficient computation of the axial irradiance in the image space provided by optical systems with any rectangular pupil transmittance. It makes use of the Wigner distribution function (WDF) of an azimuthally-averaged version of the pupil function of the system from which all the values of the axial irradiance can be obtained for a variable spherical aberration. A similar approach has been recently reported for the computation of the Strehl ratio in the neighbourhood of the image plane that contemplates the study of systems with radially symmetric apertures [18]. The main drawback of this method is its lack of flexibility, since a different WDF is required for the analysis of the same system with different amounts of aberration. This handicap is resolved by the technique proposed here.

In section 2, we give the theoretical basis of the method and, in section 3, we analyse the influence of the spherical aberration on the axial irradiance distribution for unstable resonators with different geometries.

## 2. Axial irradiance distribution in the focal region

Let us consider the focusing geometry represented in figure 1. A square pupil aperture with a rectangular non-centred obscuration is illuminated by a converging spherically-aberrated wave of focal length  $f$  and wavelength  $\lambda$ . This

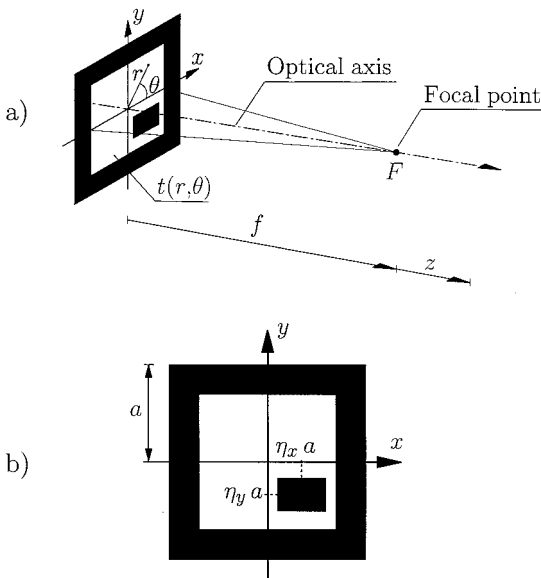


Figure 1. Schematic representation of the optical setup: (a) coordinate system, (b) relative displacement ( $\eta_x, \eta_y$ ) of the rectangular dark mask.

situation corresponds either to the field emerging from an astigmatic rectangular unstable optical resonator focalized by a converging spherical lens, or to the case in which the relative axial position of the mirrors in the unstable cavity provides an emerging focusing beam. In order to evaluate the axial amplitude distribution in the focal region, we particularize the Fresnel–Kirchhoff diffraction equation for the axial points, that is

$$U(z) = \frac{1}{\lambda f(f+z)} \int_0^{2\pi} \int_0^h t(r, \theta) \times \exp \left[ \frac{i2\pi}{\lambda} \omega_{40} \left( \frac{r}{h} \right)^4 \right] \exp \left[ -i2\pi \frac{z}{2\lambda f(f+z)} r^2 \right] r \, dr \, d\theta, \quad (1)$$

where,  $t(r, \theta)$  is the amplitude transmittance of the pupil in polar coordinates,  $\omega_{40}$  denotes the coefficient for Seidel's spherical aberration,  $h = a/2^{1/2}$  stands for the half-diagonal length of the square pupil, and  $z$  is the axial coordinate as measured from the paraxial focal point of the illuminating wave.

For our purposes it is convenient to perform two mathematical manipulations in this equation. First, the integration over  $\theta$  leads to

$$U(z) = \frac{2\pi}{\lambda f(f+z)} \int_0^h t_o(r) \exp \left[ \frac{i2\pi}{\lambda} \omega_{40} \left( \frac{r}{h} \right)^4 \right] \exp \left[ -i2\pi \frac{z}{2\lambda f(f+z)} r^2 \right] r \, dr, \quad (2)$$

where

$$t_o(r) = \frac{1}{2\pi} \int_0^{2\pi} t(r, \theta) \, d\theta, \quad (3)$$

is a continuously-varying radially-symmetric function which, at every value of  $r$ , stands for the azimuthal average of the pupil transmittance  $t(r, \theta)$  [19]. The second manipulation consists of the geometrical transformation

$$\zeta = \left( \frac{r}{h} \right)^2 - 0.5, \quad q_o(\zeta) = t_o(r), \quad (4)$$

which maps the radial interval  $[0, h]$  into the one-dimensional (1D) interval  $[-1.5, 0.5]$ , converting the integral in equation (2) into a 1D Fourier transformation of the product

$$q_o(\zeta) \exp \left( \frac{i2\pi}{\lambda} \omega_{40} \zeta^2 \right), \quad (5)$$

namely,

$$U(z) = \frac{\pi N}{(f+z)} \int_{-\infty}^{+\infty} q_o(\zeta) \exp \left( \frac{i2\pi}{\lambda} \omega_{40} \zeta^2 \right) \exp \left\{ -\frac{i2\pi}{\lambda} \left[ \frac{\lambda N z}{2(f+z)} - \omega_{40} \right] \zeta \right\} d\zeta, \quad (6)$$

where

$$N = \frac{h^2}{\lambda f}, \quad (7)$$

denotes the Fresnel number of the square aperture, which accounts for the number of Fresnel zones that are covered by the aperture as viewed from the geometrical

focus ( $z = 0$ ). In equation (6), the integration limits have been extended to infinity, provided the finite extension of the function  $q_0(\zeta)$  and an irrelevant phase factor has been omitted. The frequency variable in the above Fourier transformation can be expressed, as is usual in the image formation theory, in terms of the defocus coefficient. This parameter is defined as

$$\delta\omega_{20} = -\frac{\lambda Nz}{2(f+z)}. \quad (8)$$

Thus, the axial amplitude distribution provided by the focusing geometry at issue can be expressed as

$$U(z) = Q(\delta\omega_{20}; \omega_{40}) = \pi \left( N + \frac{2}{\lambda} \delta\omega_{20} \right) \int_{-\infty}^{+\infty} q_0(\zeta) \exp\left(\frac{i2\pi}{\lambda} \omega_{40} \zeta^2\right) \exp\left[\frac{i2\pi}{\lambda} (\delta\omega_{20} + \omega_{40}) \zeta\right] d\zeta, \quad (9)$$

and the axial irradiance distribution corresponding to a focusing geometry in the presence of spherical aberration is given by

$$\begin{aligned} I(\delta\omega_{20}; \omega_{40}) &= |Q(\delta\omega_{20}; \omega_{40})|^2 \\ &= \pi^2 \left( N + \frac{2}{\lambda} \delta\omega_{20} \right)^2 \left| \int_{-\infty}^{+\infty} q_0(\zeta) \exp\left(\frac{i2\pi}{\lambda} \omega_{40} \zeta^2\right) \right. \\ &\quad \left. \times \exp\left[\frac{i2\pi}{\lambda} (\delta\omega_{20} + \omega_{40}) \zeta\right] d\zeta \right|^2. \end{aligned} \quad (10)$$

At this point we want to remark that the axial behaviour of the focusing setup is governed by the product of two functions. The first one is a factor that explicitly depends on the value of the Fresnel number  $N$ , namely

$$\left( N + \frac{2}{\lambda} \delta\omega_{20} \right)^2. \quad (11)$$

This factor is responsible for the focal-shift effect in the low Fresnel-number geometries [2]. The second one corresponds to the square modulus of the 1D Fourier transformation of the function in expression (5), but centred at

$$\delta\omega_{20} = -\omega_{40}. \quad (12)$$

The expansion of the square modulus in equation (10) leads to

$$\begin{aligned} I(\delta\omega_{20}; \omega_{40}) &= \pi^2 \left( N + \frac{2}{\lambda} \delta\omega_{20} \right)^2 \\ &\quad \times \int_{-\infty}^{+\infty} \int_{-\infty}^{+\infty} q_0(\zeta) q_0^*(\zeta') \\ &\quad \times \exp\left\{ \frac{i2\pi}{\lambda} [(\delta\omega_{20} + \omega_{40})(\zeta - \zeta') + \omega_{40}(\zeta^2 - \zeta'^2)] \right\} d\zeta d\zeta'. \end{aligned} \quad (13)$$

Using the transformation  $x = (\zeta + \zeta')/2$  and  $x' = \zeta - \zeta'$ , equation (13) results, except for an irrelevant constant factor, in

$$\begin{aligned}
 I(\delta\omega_{20}; \omega_{40}) &= \left( N + \frac{2}{\lambda} \delta\omega_{20} \right)^2 \\
 &\times \int_{-\infty}^{+\infty} \left[ \int_{-\infty}^{+\infty} q_0 \left( x + \frac{x'}{2} \right) q_0^* \left( x - \frac{x'}{2} \right) \right. \\
 &\times \exp \left\{ \frac{i2\pi}{\lambda} [(\delta\omega_{20} + \omega_{40}) + 2\omega_{40}x]x' \right\} dx' \Big] dx, \quad (14)
 \end{aligned}$$

where the inner integral in equation (14) can be recognized as the WDF of the 1D function  $q_0$ , defined as

$$W_{q_0}(x, \nu) = \int_{-\infty}^{+\infty} q_0 \left( x + \frac{x'}{2} \right) q_0^* \left( x - \frac{x'}{2} \right) \exp(-i2\pi\nu x') dx'. \quad (15)$$

Consequently, the axial irradiance distribution can be written as a line integral of this WDF where the spatial frequency variable  $\nu$  is given by a linear function of the spatial variable  $x$  as follows

$$I(\delta\omega_{20}; \omega_{40}) = \left( N + \frac{2}{\lambda} \delta\omega_{20} \right)^2 \int_{-\infty}^{+\infty} W_{q_0}(x, m(\omega_{40})x + n(\delta\omega_{20})) dx, \quad (16)$$

being

$$m(\omega_{40}) = -\frac{2\omega_{40}}{\lambda}, \quad \text{and} \quad n(\delta\omega_{20}) = -\frac{\delta\omega_{20} + \omega_{40}}{\lambda}. \quad (17)$$

Therefore, the axial behaviour of the irradiance distribution provided by the system for any value of spherical aberration can be obtained from a single WDF of the mapped pupil  $q_0(\zeta)$ , by integrating the values of this function along straight lines in the phase-space domain. The slope and the  $y$ -intercept of these lines are given by the spherical aberration coefficient and by the wavelength through equations (17). Moreover, the same WDF provides all the information required to assess the axial behaviour of the system for any scaled version of the pupil function, since all of them lead to the same  $q_0(\zeta)$ . If the pupil of the system presents no amplitude variations, the study of the system for different values of its numerical aperture can be carried out with the same phase-space function.

### 3. Numerical examples

We have evaluated the axial response provided by three different optical systems with Fresnel number  $N = 100$ . The first one corresponds to a square clear pupil of side  $a$ . The other two systems are characterized by the same square aperture but with square obscurations located at  $(\eta_x = 0, \eta_y = 0)$  and  $(\eta_x = 0, \eta_y = 2/3)$ , respectively (see figure 1(b)). Both obscurations have sides of  $a/3$  length.

The azimuthally-averaged pupil functions  $q_0(\zeta)$  for the three systems at issue are shown in figure 2. From these functions, the three WDFs,  $W_{q_0}(x, \nu)$ , have been digitally obtained, by a sequence of fast Fourier transformations, for  $4096 \times 4096$  points in the phase-space domain. In each case, the axial values of the irradiance

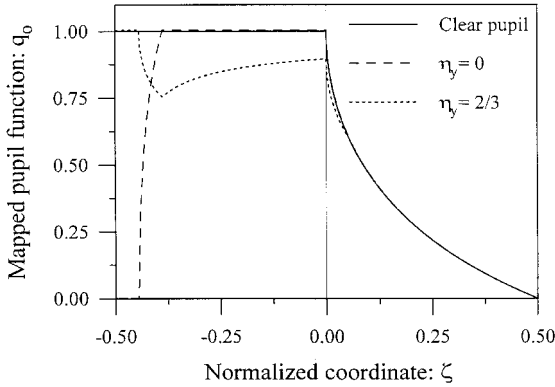


Figure 2. Mapped pupil functions for the three systems at issue.

have been achieved for different amounts of spherical aberration by numerical integration along the straight lines defined by the parameters  $\delta\omega_{20}$  (axial location) and  $\omega_{40}$  (amount of spherical aberration) by use of equations (17).

The obtained results are represented in figure 3 for five particular values of the spherical aberration coefficient, ranging from  $\omega_{40} = -2\lambda$  to  $\omega_{40} = 2\lambda$ . Regardless of their resemblance, some important features can be inferred from these representations. First, the axial irradiance distribution becomes more and more non-symmetrical with respect to its maximum value as the amount of spherical aberration increases. This fact can be explained from the characteristics of the product in expression (5), which is Fourier transformed in equation (10). For the case  $\omega_{40} = 0$ , the above product is a positive real function for all three cases under study, and therefore the square modulus of its Fourier transformation is an even function with maximum value at the origin (solid line in figure 3). For  $\omega_{40} \neq 0$ , expression (5) becomes a complex function. As the spherical aberration coefficient increases in modulus, the loss of the symmetry of its Fourier transformation becomes more noticeable.

Second, the axial maxima are shifted from the paraxial focus for values of  $\omega_{40} \neq 0$ . This shift is shown, as a function of  $\omega_{40}$ , in figure 4 for the three systems at issue. Two different regions can be observed in these representations. In the neighbourhood of the value  $\omega_{40} = 0$  these functions present a linear behaviour, whereas for a higher amount of spherical aberration they show an evident non-linear dependence. The profile of expression (5) can be used again to account for this behaviour. If the maximum value of the square modulus of its Fourier transformation remains located at the origin for  $\omega_{40} \neq 0$ , the axial irradiance peak will be located at positions that follow the linear distribution indicated in equation (12). For symmetrical  $q_0(\zeta)$  functions, this situation occurs for small values of  $|\omega_{40}|$ . If  $q_0(\zeta)$  is a shifted version of a symmetrical function, an additional linear shift is present, as has been already reported in [10]. The behaviour of the three considered mapped pupils is quite similar to this class of functions for low spherical aberration, especially for the case of the centrally obscured pupil which is a nearly-symmetrical shifted function (see figure 2). For higher values of  $\omega_{40}$ , the nonlinearity of the above axial shift is caused by the displacement of the maximum value of the square modulus of the Fourier transformation in equation (10).

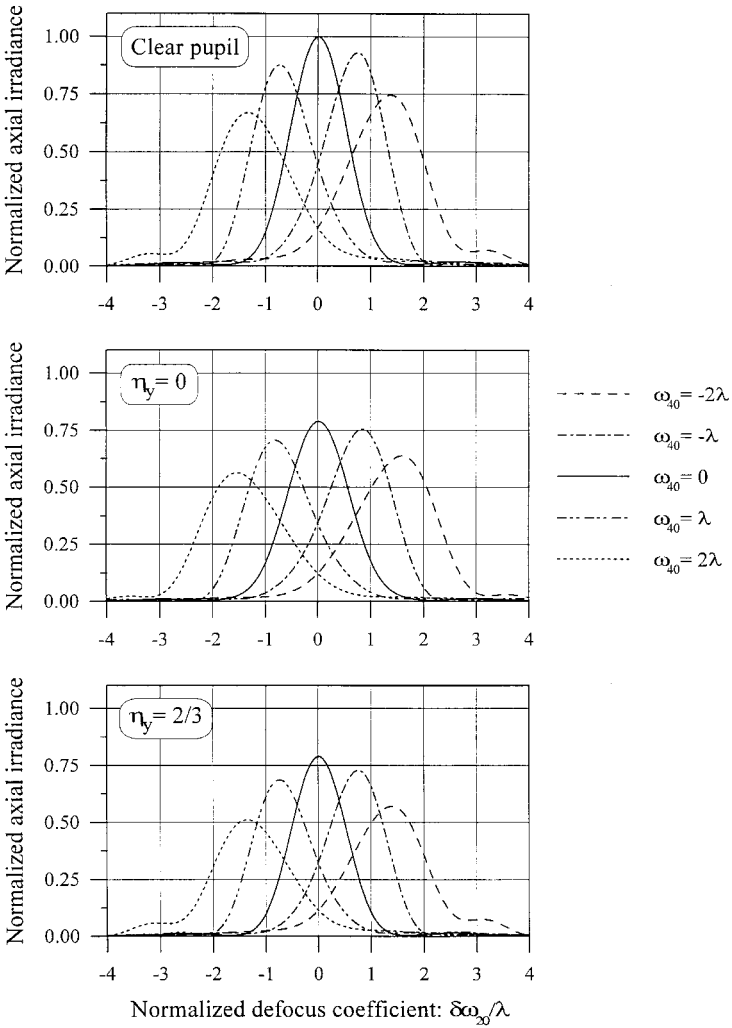


Figure 3. Normalized axial irradiance obtained from the WDF of the functions shown in figure 2, for different amounts of spherical aberration (at right). The normalization is such that the maximum value of the irradiance for the clear aperture is unity.

The third feature that can be extracted from figure 3 is that the irradiance maxima obtained for negative values of  $\omega_{40}$  are higher than those corresponding to the same amount of positive spherical aberration. This behaviour is caused by the external parabolic factor in equation (13). This would be a surprising fact because, as we are dealing with focusing systems having high Fresnel-number, it was expected that the effect of this factor would not be noticeable [1]. However, when we deal with axial irradiance patterns that are not centred at the geometrical focus, the influence of the external parabolic factor is, even for high values of  $N$ , rather different for different axial positions of the irradiance peaks, as was pointed out in [3], this being higher for the positive values of  $\delta\omega_{20}$  than for the negative ones. Since this effect becomes more significant for lower values of the Fresnel number

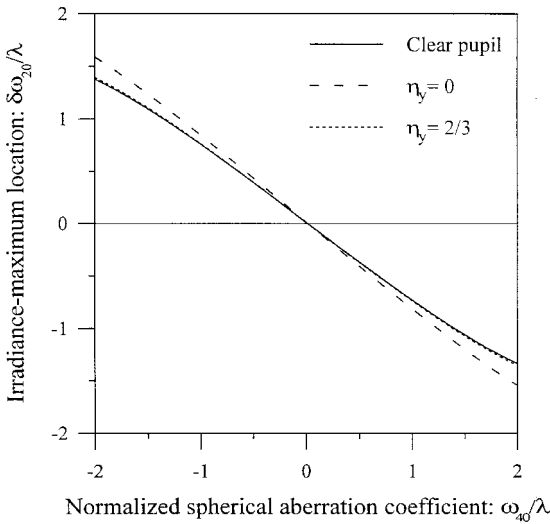


Figure 4. Axial location of the irradiance maxima as a function of the primary spherical aberration coefficient that affects the systems under study.

of this setup, it follows that it is possible to design optical systems in which the combination of a given amount of spherical aberration with a proper Fresnel number provides an overall irradiance peak higher than the one obtained with the aberration-free situation. This is an interesting effect that, to our knowledge, has not been reported before in the literature.

Finally, it is noticeable that, except from the obvious decrease in the maximum irradiance values, both the shape (figure 3) and the maxima location (figure 4) of the axial irradiance distribution provided by the systems with clear and decentered pupils are quite similar, while the case with central obscuration departs from this common behaviour. This effect can be explained by the inspection of figure 2 if one realizes that in the first two cases both mapped functions  $q_o(\zeta)$ —and, therefore, their WDF representations—are much more similar to each other than to the third one.

#### 4. Conclusions

The influence of the spherical aberration on the axial irradiance produced by focusing optical systems with obscured square apertures has been investigated. The analysis of the irradiance along the optical axis has been performed with an original method that uses the WDF of a 1D function, which is directly derived from the pupil function of the system. This method is especially adapted to the study presented here, because all the axial irradiance values can be obtained from the same phase-space function for a variable spherical aberration, provided that the coefficient corresponding to this aberration is a parameter in our approach.

From the above analysis several interesting features have been extracted. First, the profile of the irradiance distribution along the optical axis is non-symmetrical around its maximum value for spherically aberrated systems. Second, the overall axial maxima are shifted from the paraxial focal point in an almost linear fashion.

Third, the magnitude of these maxima depends not only on the modulus of  $\omega_{40}$  but also on its sign. All these features have been interpreted in terms of the characteristics of the above-mentioned 1D function associated with the pupil of the system.

Finally it is worth mentioning that the method used in this work is not restricted to the application presented here. Since the wavelength is also a parameter in the computation of the axial irradiance distribution, it can be successfully applied to the computation of quality parameters for optical systems working under polychromatic illumination. A similar approach has already been used in computing polychromatic merit functions [20].

### Acknowledgments

This research has been supported by the Universitat de València (Projectes Precompetitius d'Investigació 1994). E. Silvestre gratefully acknowledges the financial support of the Dirección General de Investigación Científica y Técnica (grant PB-0354-C02-01), Ministerio de Educación y Ciencia, Spain.

### References

- [1] LI, Y., and WOLF, E., 1981, *Optics Commun.*, **39**, 211.
- [2] MARTÍNEZ-CORRAL, M., ANDRÉS, P., and OJEDA-CASTAÑEDA, J., 1994, *Appl. Optics*, **33**, 2223.
- [3] MARTÍNEZ-CORRAL, M., and CLIMENT, V., 1996, *Appl. Optics*, **35**, 24.
- [4] LOHMANN, A. W., and OJEDA-CASTAÑEDA, J., 1984, *Optica Acta*, **31**, 603.
- [5] MAHAJAN, V. M., 1983, *Appl. Optics*, **22**, 3042.
- [6] OJEDA-CASTAÑEDA, J., and BERRIEL-VALDOS, L. R., 1988, *Optics Lett.*, **13**, 183.
- [7] SHEPPARD, C. J., and HEGEDUS, Z. S., 1988, *J. opt. Soc. Am. A*, **5**, 643.
- [8] YZUEL, M. J., ESCALERA, J. C., and CAMPOS, J., 1990, *Appl. Optics*, **29**, 1631.
- [9] MARTÍNEZ-CORRAL, M., ANDRÉS, P., OJEDA-CASTAÑEDA, J., and SAAVEDRA, G., 1995, *Optics Commun.*, **119**, 491.
- [10] OJEDA-CASTAÑEDA, J., TEPICHIN, E., and PONS, A., 1988, *Appl. Optics*, **27**, 5140.
- [11] GEARY, J. M., and PETERSON, P., 1986, *Opt. Eng.*, **25**, 286.
- [12] GONG, Q., and HSU, S. S., 1994, *Opt. Eng.*, **33**, 1176.
- [13] SUTTON, G. W., WEINER, M. M., and MANI, S. A., 1976, *Appl. Optics*, **15**, 2228.
- [14] MAHAJAN, V. M., 1978, *J. opt. Soc. Am.*, **68**, 742.
- [15] FRIEDMAN, E., 1992, *Appl. Optics*, **31**, 14.
- [16] OJEDA-CASTAÑEDA, J., MARTÍNEZ-CORRAL, M., ANDRÉS, P., and PONS, A., 1994, *Appl. Optics*, **33**, 7611.
- [17] SIEGMAN, A., 1986, *Lasers* (Mill Valley: University Science Books), p. 901.
- [18] ZALVIDEA, D., LEHMAN, M., GRANIERI, S., and SICRE, E. E., 1995, *Optics Commun.*, **118**, 207.
- [19] MCCUTCHEM, C. W., 1964, *J. opt. Soc. Am.*, **54**, 240.
- [20] FURLAN, W. D., SAAVEDRA, G., SILVESTRE, E., YZUEL, M. J., and ANDRÉS, P., 1996, *Proc. SPIE*, **2730**, 252.

